IEEE JOURNAL OF

QUANTUM ELECTRONICS

A PUBLICATION OF THE IEEE PHOTONICS SOCIETY

IEEE photonics SOCIETY

This Print Collection Contains the Following Issues:

MAY 2012	VOLUME 48	NUMBER 5	IEJQA7	(ISSN 0018–9197)
JUNE 2012	VOLUME 48	NUMBER 6	IEJQA7	(ISSN 0018–9197)

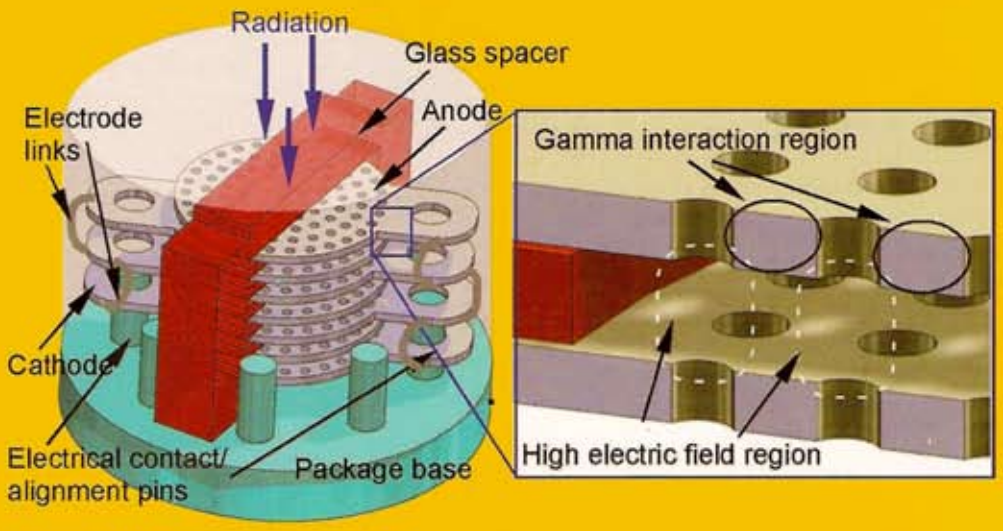

Radiation detector concept. The detector comprises a stacked arrangement of multielectrode stainless steel elements (i.e., anode and cathode) and a glass insulator, assembled within a commercial TO-5 package base. Each electrode is an array of three or four "linked" elements. Machined shelves in the spacer maintain a 200-μm-wide interelectrode spacing between each electrode layer. Gamma radiation interacts with the metal layers, which releases photoelectrons into the biased gap. These charged particles trigger an avalanche within the biased gap, leading to wireless signaling (Eun and Gianchandani, p. 822).

For the May 2012 issue, see p. 557 for the Table of Contents.
For the June 2012 issue, see p. 735 for the Table of Contents.

IEEE

Microdischarge-Based Sensors and Actuators for Portable Microsystems: Selected Examples

Christine K. Eun and Yogesh B. Gianchandani, *Fellow, IEEE*

(Invited Paper)

***Abstract*— This paper describes the use of microdischarges as transducing elements in sensors and actuators. Chemical sensing of gases and liquids, pressure sensing in harsh environments, on-chip pressure regulation, and radiation detection methods are described. The devices targeted for these applications are presented from the perspective of the ease of integration into portable microsystems, with emphasis on compactness, power consumption, and the ability to operate over a wide range of temperatures and pressures. Performance results and other important integration considerations, such as manufacturing approaches and device packaging methods, are described for selected examples.**

***Index Terms*— Chemical, discharge, plasma, pressure, radiation, sputter-ion pump.**

I. Introduction

In THE past decade, micro-scale plasmas, or more generally, microdischarges, have been explored for fundamental properties, and employed in a variety of sensing and actuating devices. There are a variety of important applications that can be addressed by plasma-based microsystems. For example, homeland security motivates research in portable analytical systems, such as those needed to identify and quantify the chemical composition of unknown substances. Another example is environmental surveillance e.g., monitoring radiation levels. Integrated microsystems can be deployed in networked configurations to remotely monitor large areas and provide real-time alerts. These types of implementations typically require stand-alone operation, which entails miniaturized sensor and actuator structures, battery-powered operation, and in many cases, even miniaturization of the entire system. The design of such integrated microsystems must take into account transducer features e.g., power, footprint, weight, and packaging. As a consequence of certain scaling benefits, microdischarges can offer attractive options for many such sensing and actuation needs.

Microdischarges, which for the purpose of this paper include plasmas, arcs, and sparks, utilize electrodes and spacings in the micron-to-millimeter scale. Compared to conventional plasmas, such as those used in semiconductor processing equipment, microdischarges can operate at pressures easily exceeding atmospheric pressure. Another consequence of miniaturization is that very high power densities can be achieved without requiring high power: while conventional plasmas may operate at 10-500 mW/cm^2 of electrode area, microdischarges can be operated at power density levels that are larger by several orders of magnitude. Volumetric power densities in the tens of kW/cm^3 and up to 1 MW/cm^3 have been reported [1-4]. Electron temperatures in microdischarges can also be relatively high, reaching 5-6 eV in small percentages of very high-energy beam electrons [1, 2, 5, 6]. Additionally, the relatively large ratio of surface area to discharge volume can make wall interactions more prominent. For example, in direct current (DC)-powered microdischarges, the ionization is dominated by secondary electrons, and the glow region, which is proximal to the cathode, may overlap the high field region. Further distinctions between conventional and micro-scale discharges are reviewed in [1, 2, 6].

One promising application area for microdischarge-based devices is chemical sensing. Miniaturized and portable systems for gas and liquid sensing can address applications ranging from environmental monitoring to homeland security. The emission spectrum of a discharge arises from spontaneous emission due to relaxation of excited chemical species to the ground states. In principle, a single observation of a pulsed discharge can provide information regarding the composition of the ambient gas mixture. With modifications, emission spectroscopy of microdischarges can be extended to liquid-phase ambients.

Microdischarges can enable pressure sensing in high temperature environments over a wide range of pressure. Devices utilizing microdischarges are suitable for high temperature operation because the electrons and ions have average energies in the range of 1-3 eV [1-8] and >0.03 eV, respectively, in an ambient environment. These temperatures allow the species to be only minimally affected by a high or low temperature ambient, making it possible for microdischarge-based devices to operate at temperatures in excess of 1,000 °C and potentially down to cryogenic temperatures. One approach exploits the variation in the mean free path of gas molecules as a function of pressure [3, 9]. Another method measures the deflection of a diaphragm electrode resulting from an external pressure. The diaphragm serves as a second cathode in conjunction with another fixed cathode. When deflected, the distance between the anode and the deflected diaphragm is affected, altering the current distribution of microdischarges between the two cathodes with pressure.

Manuscript received November 9, 2011; accepted February 22, 2012. Date of publication February 27, 2012; date of current version May 1, 2012. This work was supported in part by the National Science Foundation, the Sea Grant Institute, the Water Resources Institute, and the Advanced Energy Consortium.

The authors are with the University of Michigan, Ann Arbor, MI 48197 USA (e-mail: eunc@umich.edu; yogesh@umich.edu).

Color versions of one or more of the figures in this paper are available online at http://ieeexplore.ieee.org.

Digital Object Identifier 10.1109/JQE.2012.2189199

There are other interesting applications for microdischarges. For example, these can also be used for controlling pressure in microsystem packages. Macro-scale sputter-ion-pumps (SIPs) operate through the creation of discharges in externally applied magnetic fields, which trap electrons and ionize the surrounding gases. Ions, which are then accelerated toward the cathode, sputter fresh titanium onto the surrounding walls and anode. The titanium getters both nitrogen and oxygen [10-15]. Miniaturized versions operate similarly but do not require external magnetic fields, except at very low pressures. Gas discharges have also been employed in radiation detection e.g., in Geiger counters and proportional counters. Miniaturized versions of these detectors utilize microdischarges. These micro-scale discharges have been shown to generate wideband wireless transmissions existing in the ultra-wideband (UWB) frequency band [16, 17].

This paper explores how microdischarges can be used as a transduction element in different domains. Section 2 describes the gas-phase and liquid-phase sensing of chemical species using emission spectroscopy. Section 3 describes discharge-based pressure sensing in extreme environments such as high pressures and temperatures. Section 4 describes the use of microdischarges to getter gas molecules in confined volumes, both for pressure regulation in microcavities and the purification of gas samples in miniature chemical sensors. Section 5 describes gas-based radiation detection and the exploration of micro-scale plasmas as radio-frequency transmitters. All microdischarge-based transducers that are reviewed here have some feature sizes with sub-millimeter dimensions, and are typically microfabricated. To the extent possible, all applications are explored from the perspective of microsystems, with emphasis on device compactness and power consumption; and will address important systems-level considerations such as packaging approaches.

II. Discharge-Based Chemical Sensing

Microsystems capable of gas-phase sensing over a range of environmental conditions are important for various monitoring applications e.g., the fuel composition in automotive systems and the air quality in aeronautic and space vehicle systems. Water analysis also provides an opportunity: with the mounting challenges of supplying potable water to the growing population of the world, low cost and portable microsystems can be envisioned for point-of-use analysis. Liquid-phase chemical sensing has been explored primarily in the context of testing water for inorganic impurities.

A. Gas-Phase Chemical Sensing

Microdischarges can be used for gas-phase chemical sensing by a variety of analytical techniques including, optical emission spectroscopy, plasma mass spectrometry, and ion mobility spectrometry. In contrast with conventional gas sensors that depend on the absorption of selected analytes, spectroscopic sensors allow the rapid and concurrent sensing of multiple species. This is because the entire spectrum can be captured in a single snapshot and also because microdischarges can fluoresce many species simultaneously. In addition, the generation of these microplasmas tends to be less sensitive to operating temperatures and variations in fabrication [18, 19].

Gas-phase sensors can utilize a variety of DC and radio-frequency (RF)-powered microdischarges [18-26]. RF-powered microplasmas include miniature inductively coupled plasmas (ICP), microwave induced plasmas (MIP), capacitively coupled plasmas (CCP), dielectric barrier discharges (DBD), and microhollow cathode discharges (MHCD). The majority of the structures used to generate these RF plasmas utilizes a dielectric layer between the electrodes and the plasma region, which prevents sputtering of the electrodes. DC-powered discharges can include DC microplasmas using planar electrode configurations, pulsed micro-arcs, three-electrode microdischarges, arc-glow hybrid microdischarges, and multi-cathode pulsed DC microdischarges. These typically require less external hardware for operation compared to RF-powered transducers, and are more amenable to miniaturization and battery-powered operation. Although DC-powered microdischarges heat the electrodes to a greater extent compared to RF-powered microdischarges, the lifetime of DC-powered transducers can be extended by utilizing pulsed discharges. This paper focuses more closely on DC microplasmas with the exception of arc-glow hybrid microdischarges, which have been further studied here [27].

DC discharges that operate in inert gases at atmospheric pressure have been used for optical emission spectroscopy. A macro-scale discharge was used at the end of gas chromatographs (GCs) as far back as 1968 [28]. GCs are amongst the most powerful analytical instruments available today for the separation and identification of mixtures of gases. Post-separation, sensing or detection can be performed by a variety of means ranging from mass spectrometry to simple thermal flow sensors. Recent efforts to miniaturize GCs [29, 30] present opportunities for integration with microdischarge-based transducers. An early paper describes a microplasma mass spectrometer coupled to a GC for halogen detection [31]. A review of the use of microdischarge-based transducers with GCs has been presented by Miclea and Franzke [19-21].

One of the earliest microdischarge-based gas-phase sensor was reported by Manz's group [32]. It utilized DC microplasmas between planar electrode geometries in a helium environment. Chambers of varying dimensions and volumes were fabricated by fusion bonding a glass chip with a recessed cavity to another chip with patterned metal electrodes. Microplasmas were created between 50-150 Torr in a 50 nl chamber, which required 6 kV for ignition. Approximately 50 mW power was dissipated in the plasma, with additional power dissipated in the 90 MΩ ballast resistor. An external spectrometer was used for detection. Using this device, methane was detected with a detection limit of 600 ppm by observing the CH diatomic emission band. Enhanced operation was reported in a subsequent effort [33], detecting 50 ppm of methane in a helium background. The device was also coupled to a GC [34].

Another DC-powered gas-phase sensor utilized two coaxial tungsten wire electrodes (50 μm diameter, 2 mm separation) inserted into a fused silica capillary (250 μm inner diameter, 8 cm length) [35]. This wire electrode design was expanded to encompass four pairs of tungsten wire electrodes with tips

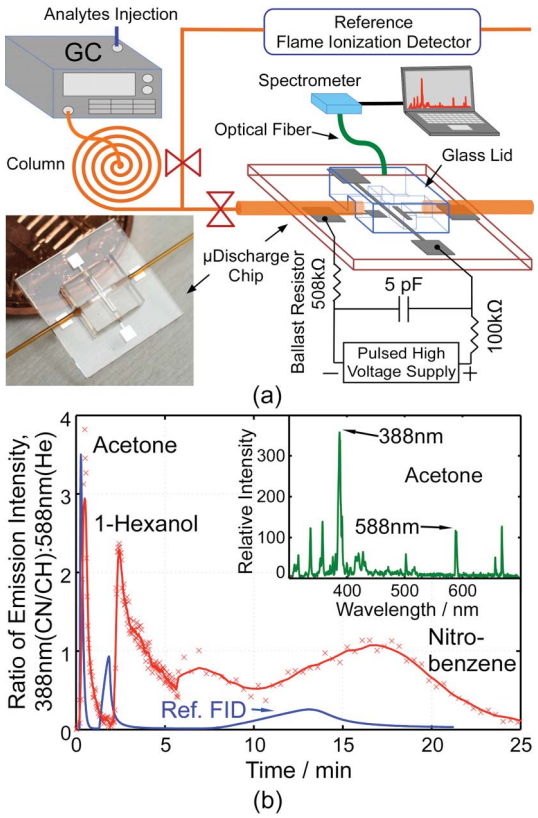

Fig. 1. (a) Schematic of a microfabricated, pulsed discharge-based chemical sensor for gas species. The device was coupled to a GC separation column and read out by a spectrometer. (b) Chromatograms obtained from the microdischarge response and reference FID. Inset: typical pulsed spectrum with enhanced 388-nm peaks, representing CN/CH fragments [37].

2 mm apart on a microfabricated chip (25 mm × 15 mm). Gas flowed through an etched channel in which the microplasmas were generated. Chlorine was detected with a detection limit of 8×10^{-10} g/s using the 479.5 nm emission line. Typical discharge voltages were 600 V and the minimum utilized power was 260 mW.

A device utilizing two planar DC microplasmas on a single chip, the first serving as an injector to a GC and the second as an ionization source following the columns, has been reported [36]. Samples of $CHCl_3$ and CH_2Cl_2 were introduced with background helium to the first injector microplasma, which was sustained except during brief intervals. In this way, it continually ionized and fragmented the molecules in the original sample. The level of fragmentation was controlled by the plasma parameters, such as electron energy, ion energy, and current density. This control allowed modulation of the flux of gas in the stream. When the plasma was briefly interrupted, it introduced a "plug" of unmodified sample into the system. Plugs between 5 ml and 50 ml were sent through the system, modulating the sample introduced into the columns. After separation in the columns, the samples were ionized and excited by the second microplasma device that was coupled to a spectrometer. The voltages applied to generate the plasmas were typically in the range of 1 to 2 kV. The detection limits for $CHCl_3$ and CH_2Cl_2 were approximately 1 μg/l. Two versions of the microplasma-based devices were fabricated; one used planar electrodes on a chip and a second used wire electrodes in a capillary as previously discussed. Device lifetime was limited by surface and electrode contamination.

The majority of the work in discharge-based chemical sensing has focused on DC-powered, steady-state plasmas. Pulsed DC powering can be attractive for a number of reasons: 1) lower power and energy consumption, that ultimately increases device lifetime and allows battery operation, and 2) the use of transient emissions for enhanced spectral analysis. Pulsed micro-arcs are particularly attractive because these high temperature discharges can provide an intense glow, with spectral emission from ultraviolet (UV) to infrared.

Pulsed micro-arcs were used in a discharge-based chemical sensor, which operated at atmospheric pressure in air [27]. The microdischarges were created between two planar electroplated copper electrodes on a Pyrex substrate. Typical emission spectra were comprised of peaks corresponding to atmospheric gases, superimposed on a broadband background. The temporal evolution of the emitted spectra was used to partially separate the broadband background, which had different afterglow characteristics than the emission peaks.

The use of pulsed microdischarge spectroscopy for GC has been reported recently [37]. A 1 cm^2 glass chip with thin-film Ni electrodes separated by 160 μm was coupled to a GC (Fig. 1a). A glass lid with a grooved gas-flow channel, and inlet/outlet capillary tubes were epoxy-sealed to the chip. Located downstream of the 1.7 m-long, RTX-1-coated, GC separation column, the microdischarge chip was read by a spectrometer. In a typical experiment (Fig. 1a), a mixture of 3.6 μg acetone, 2.8 μg 1-hexanol, and 3.0 μg nitrobenzene with a He carrier gas was injected through the GC. Acetone eluded rapidly, while nitrobenzene was slower. Microdischarges were triggered at 0.5 Hz for 6 min. and 0.04 Hz, thereafter. Each microdischarge consumed ≈8 mJ; the average power was ≈1.14 mW. The spectrum (Fig. 1b, inset) showed that the 388 nm peak, representing CN/CH fragments [38], was enhanced by carbon compounds. Its strength relative to the 588 nm peak of He provided a chromatogram. Fig. 1b also shows a benchmark result from a commercial flame ionization detector (FID). The differences in elution time were attributed to differences in the gas flow paths for the two detectors [33, 34].

In addition to pulsing the microdischarge, power savings can be achieved by the use of multi-electrode configurations. These schemes also offer a means of controlling discharge energy, and thereby tailoring the emission spectra. A three-electrode (flashFET) microdischarge device was reported by Mitra *et al.* [39]. The flashFET (Fig. 2) utilized pulsed discharges and had two structural differences from the previously described planar two-electrode DC structures: 1) it used a strategically located high-impedance electrode with a fixed bias and 2) one of the two low impedance electrodes was capacitively powered to limit the discharge energy. Analogous to a field-effect transistor (FET), the high impedance electrode was labeled the gate, the capacitively driven electrode was anodically biased and was labeled the drain, and the third electrode was cathodically biased and labeled the source. The drain was located next to the source, with a typical spacing of

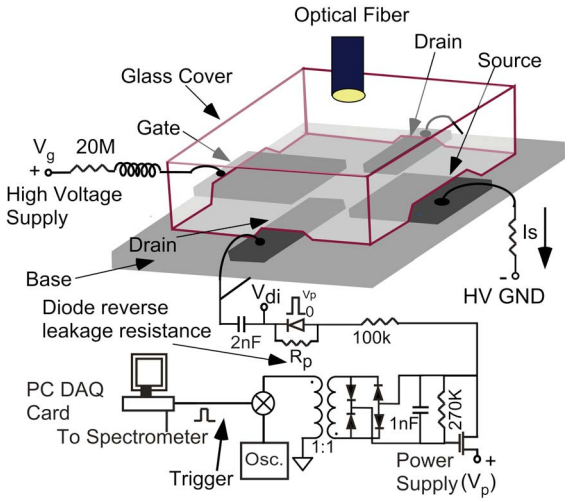

Fig. 2. Schematic of the three-electrode flashFET, showing the electrode configuration, the glass cover, and the discharge circuit. The gate is held at a high voltage, but the current is restrained by a large resistor and choke. The reverse leakage resistance of the diode allows the series capacitance at the drain to charge up in the absence of a microdischarge. A low-voltage (≈100 V) pulse is used to trigger the microdischarge at the drain end [39].

200 μm, and the gate was further away, spaced 450 μm from the source.

The current through the gate electrode was constrained by a large series resistor. The drain electrode was floating, which allowed it to charge up to a level between the gate (held at 800-1000V) and source potentials. The energy stored in the drain-source capacitor was discharged by applying a small voltage pulse to the drain (≈100V), which caused the potential to rise above the breakdown threshold. This approach reduced the energy/pulse by as much as 100× compared to a similar two-electrode microdischarge. For example, a planar two-electrode device with a 200-μm discharge gap required 0.47 mJ over a duration of 6.5 ms, whereas the three-electrode flashFET with a 200-μm drain-source spacing and a 450-μm gate-source spacing required 2.5 μJ over a duration of 200 μs, when operated at atmospheric pressure [39]. In preliminary tests, the monolithic flashFET was used to detect carbon in organic vapors using the 388.1 nm CN emission line. The line intensity was normalized to the nitrogen emission line (391.4 nm). Concentrations of 50 ppm were detected.

A handheld system that utilized microdischarges between two or three planar copper electrodes was reported in [27]. The system included a holder for microchips on which the discharge electrodes were located; chips suitable for both gas-phase and liquid-phase samples could be accommodated. A custom circuit provided pulses of controlled delay and duration for the microdischarges and synchronized data acquisition. A miniature spectrometer was used to capture the optical signals and to transfer the data to a wireless-enabled personal digital assistant (PDA). The system was powered by rechargeable 3.6-V Li-ion batteries, allowing for stand-alone operation. The 388.6 nm CN emission line, produced from acetone vapor, was used for detection and a response curve was measured. The device was able to detect 17 ppm of acetone vapor in air at atmospheric pressure, without any pre-concentration of vapors.

B. Liquid-Phase Chemical Sensing

The detection and measurement of inorganic species in water has been performed by emission spectroscopy on a water sample that was sprayed into an ICP. Other options include the use of FET devices with ion sensitive gate materials to analyze certain ionic species such as [40], which are not discussed in this review. The promise of high sensitivity and selectivity has motivated efforts to miniaturize spectroscopic devices. A micromachined four pole electrostatic lens mass spectrometer and an RF ion mobility spectrometer have been reported [41, 42]. Research toward analyzing water impurities using microdischarge-based spectroscopy has also been reported [18].

A device reported by Jenkins and Manz utilized a planar glass chip for sample containment with an attached peristaltic pump for water sample analysis [43]. A wire-based Pt anode (100 μm-diameter), which reduced wear and allowed anode repositioning, potentially allowed for long discharge time cycles. The discharge voltage and current were approximately 1 kV and 1-5 mA, respectively, and the device utilized 1-5 W power. It was operated in an argon ambient, which reduced the background signals resulting from nitrogen and molecular oxygen constituents in air. The system was shown to detect Cu in 0.1-M solution of $CuSO_4$; however, there were concerns about the stability of the plasma.

A similar strategy was followed in a device reported by Cserfalvi and Mezei, creating an electrolyte cathode glow discharge (ELCAD) [44]. The ELCAD used a capillary tube (with an inner and outer diameter of 1 mm and 5 mm, respectively) with an electrolyte conductor at the cathode, and a 1.6 mm tungsten wire as the anode. This allowed physical control of the anode-cathode spacing, which ranged between 1.5-2.5 mm. The device also allowed for control of the flow rate of the liquid under test, which extended lifetimes and increased discharge stability. The device used 82 W power, while operating in air at atmospheric pressure. The open circuit voltage was set to 1200 V, and current was set between 30-100 mA. Detection limits of 14-34 ppb were realized for Cd, Zn, Cu, Pb, and Ni.

Another glow discharge device used liquid as the cathode with an open air discharge [45]. It utilized a 3 mm outer diameter Pt rod suspended 1 mm over the cathode aqueous solution. A stable discharge was obtained when operated at 1500 V and 80 mA. The detection of a wide variety of contaminants was reported in the 10-30 μg/l range, including Cu, Fe, Mn, Ni, and Pb. This performance makes the system potentially useful for the monitoring of drinking water supplies.

Microplasma devices (MPDs) capable of analyzing liquid and powdered solid analytes at atmospheric pressure were reported by Karanassios [46, 47]. A new method of detection was explored that coupled an electrothermal, mini-in-torch vaporization (mini-ITV) "dry" sample-introduction system to the MPDs. AC-powered microdischarges appreciably extended the electrode lifetimes. Detection limits for this apparatus were reported as 2 pg for K, and 25 ng for Pb. The mini-ITV also enabled measurement of analyte emission from microsamples of powdered solids in the form of slurries.

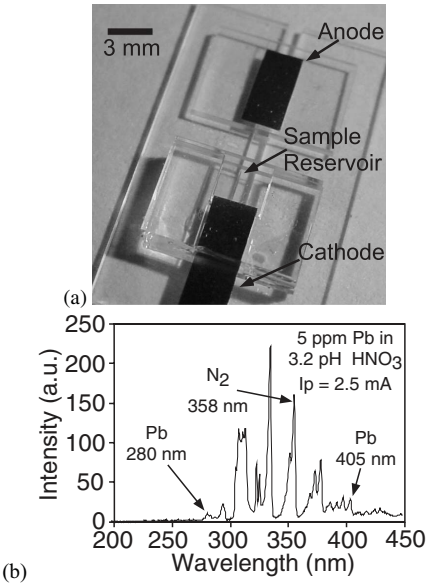

Fig. 3. (a) Photograph of a structure used for the detection of inorganic impurities in water samples by emission spectroscopy of microdischarges [51]. The test sample is cathodically biased and resides in a reservoir that leads to the microdischarge region through a channel. The anode can be a thin-film metal feature or another liquid sample. (b) Sample emission spectrum from an aqueous sample containing 5 ppm of Pb [50].

A liquid sampling–atmospheric pressure glow discharge (LS-APGD) transducer for optical emission spectroscopy was reported by Davis and Marcus [48]. This device again utilized a liquid solution as an electrode. The delivery of the impurities was performed by local heating and volatilization, so the liquid could be either the anode or the cathode [49]. The use of heating to deliver impurities required higher currents (approx. 80 mA) than other systems. However, the atmospheric discharge, which operated at these higher powers, was found to be more stable than other discharges. Analysis of the I-V curves of the discharge showed operation in the abnormal plasma regime. (This regime traditionally offers higher current densities and increased plasma heating compared to the normal glow regime.) Analytical response curves for Hg, Mg, Na, and Pb were demonstrated to have good linearity, with limits of detection reported to be 1.1–2.0 ppm for 5 μL sample volumes.

A liquid electrode spectroscopic emission chip (LEd-SpEC) that miniaturized a significant number of components was reported [50]. The LEd-SpEC utilized a pulsed DC micro-arc in air at atmospheric pressure (Fig. 3a). This device was fabricated on a glass substrate, which featured an etched recess for the water reservoir and delivery channel, and patterned thin-film Pt electrodes. The discharge was triggered between a wet cathode and an anode that was similarly wet or an anode that was dry metal. The interelectrode spacing ranged from 0.5-3 mm, while operating voltages ranged between 1.1-2.1 kV. It was shown that water and impurities were sputtered into the glow discharge region from the cathode alone. The liquid sample was delivered from an on-chip reservoir to the discharge region along a polymer-covered channel with an embedded thin-film metal lead for biasing. (Alternatively, the cathode could be a porous material that wicked the water sample from the reservoir [27].) The use of a liquid-covered cathode also eliminated the problem of electrode wear. An optical fiber mounted proximate to the discharge delivered the optical signal to a pager-sized spectrometer, connected to a data acquisition computer. LEd-SpEC devices and several variants were used to detect Pb, Cr, Al, and Na. Typical spectra obtained with a 5-ppm sample of Pb in a solution containing nitric acid showed reduced pH levels as low as 3.2 (Fig. 3b). The characteristic emission lines at 280 nm and 405 nm were evident. Samples of Cr and Al at similar concentrations were also detected. The LEd-SpEC device was also shown to be reusable: after measuring Na samples, then cleaning with DI water, no residual spectral signals were detected. To enable multiple water samples to be tested simultaneously, it is possible to integrate the dispersion optics of the spectrometer directly on the microdischarge device, so that a simple digital image can be used to perform the analysis [51].

To compensate for potential variations in the power density of the microdischarges, it is appropriate to use a differential sensing approach. One option is to use the emission intensity ratio of the target impurity to that of a signature nitrogen emission line from the air ambient. Wilson reported this approach in [50]: the ratio of intensities for the sodium emission line to the 358 nm nitrogen emission line ranged from 0.24 for 10-ppm Na, to 3.2 for 1000-ppm Na. This resulted in a log-linear response curve over several orders of magnitude, as the spectral intensity of the nitrogen emission line remained relatively constant. With the use of an appropriate pre-concentration method, it can be expected that detection limits of microdischarge-based transducers, such as LEd-SpEC, can easily be improved to 10-100 ppb levels. Another option for differential sensing is to use an internal chemical reference that was added to the test sample [52].

Miniaturized optical sources can enable on-chip fluorescence detection for applications such as biochemical analysis or medical diagnostics. Microdischarges have shown promising emission characteristics in the UV region [53]. Aqueous cathodes can provide emission spectra that are characteristic of the dissolved inorganic impurities. One configuration that has been reported includes a stacked structure of bonded glass layers. A strip of metal foil was used as the anode for its superior wear-resistant properties. The biochemical reservoir containing a saturated salt solution served as the cathode. The discharge gap was 400 μm. When the microdischarge was ignited, the ions in the aqueous cathode were sputtered into the glow region of the discharge and emitted a characteristic glow. Unwanted wavelengths were rejected by an optical filter that separated the microdischarge from the fluorescent sample. A dichroic color filter was chosen as the integrated band pass filter due to its low sensitivity to the light incident angle and its robustness. The sample was located in a reservoir or channel. The filtered emission from the discharge pulse stimulated fluorescence in the sample reservoir. In general, this could be part of a larger microfluidic network e.g., a micro-total analysis system. A photograph of the assembled device is shown in Fig. 4.

This device was demonstrated as a UV source for the detection, by fluorescence, of unlabeled tryptophan and dye

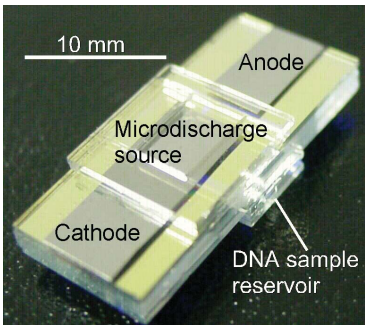

Fig. 4. Photograph of a micromachined optical source for fluorescent detection. The chip is held vertically during operation [53], [54].

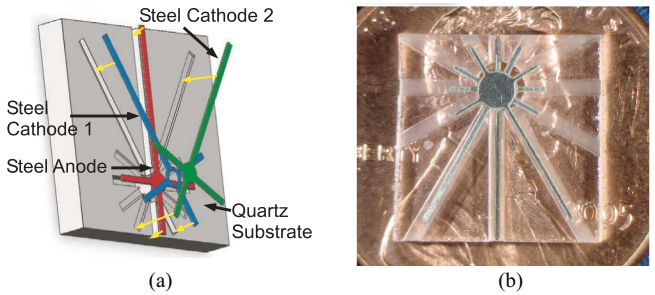

Fig. 5. (a) Sensor schematic with electrodes above a quartz chip, illustrating placement, and the microdischarge chamber during operation. (b) Sensor photograph on a penny [3], [9].

labeled DNA. In particular, a solution of $Pb(NO_3)_2$ was used to generate an emission at 280 nm, which is close to the absorption peak of tryptophan. In another example, a $BaCl_2$ solution was used to generate peaks at 453 nm and 493 nm, which are close to the excitation peaks for DNA tagged with SYBR green dye [53-55].

III. Discharge-Based Pressure Sensing

Micro-scale pressure sensors that can operate in harsh conditions (e.g., high pressures, extreme temperatures, and corrosive fluid ambients) are needed for a variety of applications. Examples include space exploration, subterranean mining, and oil wells. Additionally, such sensors can be used to monitor gas turbine engines, coil boilers, and furnaces. A variety of optical and electrical microstructures have been proposed for these applications. Optical pressure sensing approaches include Fabry-Perot cavities that respond to applied pressure [56, 57] and photo-inscribed Bragg gratings that provide wavelength shifts due to strain in optical fibers [58, 59]. The electrical transduction methods that are favored for pressure sensors are capacitive and piezoresistive. Both of these utilize deflecting diaphragms – the former to measure diaphragm displacement; the latter to measure stress. Using a Si diaphragm, operation at temperatures as high as 800°C has been reported [60]. In addition, efforts using unconventional diaphragm materials such as silicon carbide [61] and sapphire [62] have been reported. A discharge-based approach to pressure sensing is complementary to previous techniques because it provides a direct electrical readout that requires no signal conditioning or amplification. This approach is also of interest because of the potential for wide dynamic range and temperature immunity. As previously mentioned, discharge-based devices are well suited for high temperature operation because the electron and ions are only minimally influenced by ambient temperature changes.

Sensor characteristics such as the sensitivity, pressure dynamic range, and temperature dynamic range depend on a variety of dimensional parameters, including inter-electrode spacing, electrode diameter, and the cathode thickness. (Cathode thickness can impact sheath surface area as well as electrode positioning). The sensors can be designed to function with an applied voltage on the order of a few 100 V; altering the voltage can result in different sensitivities. The nature of the encapsulated gas can also impact the operating voltages.

A pulsed-DC microdischarge-based vacuum sensor that exploits the variation, with pressure, of the mean free path of gas molecules was reported [3, 9]. As gas pressure increased, the mean free path of ionized molecules was reduced, and this changed the fractional current, $(I_1 - I_2)/(I_1 + I_2)$, between two cathodes that were at different distances from the anode [8]. At low pressures, current favored the farthest cathodes, while at high pressures the opposite occurred. In principle, a multi-anode structure can be used instead of a multi-cathode structure. However, the pressure sensitivity of this arrangement tends to be too high, and the dynamic range consequently tends to be too low [8]. These sensors were different than ion gauges, which are not effective at atmospheric pressure because the small mean free path of the ions, 20-65 nm, make thermionic emissions difficult to detect [63].

The sensor structure consisted of several metal foil electrodes stacked within a machined quartz chip (Fig. 5a). A disk-shaped anode served as the bottom of the discharge chamber, the center electrodes were torus-shaped, and the top cathode was disk-shaped. In order to accommodate the wide range of operating temperatures, an arrangement that accommodated the expansion mismatch between the electrodes and substrate was necessary. The electrodes were lithographically patterned and photochemically etched from stainless steel foil [64]. Trenches of specified depths and a through-hole in the center were formed in a planar quartz substrate by a lithographically masked sand-blasting process. The electrodes were then assembled in the trenches (Fig. 5b).

The anode/cathode spacing in these sensors was set to produce measurable results up to 1,000 °C, for pressures between 10 Torr and 2000 Torr. These devices demonstrated sensitivities in the range of 5,420 ppm/Torr, for lower pressures and 500 ppm/Torr, for higher pressures. Pulses were applied at a rate of 2-10 Hz to the sensors with voltages between 700 V and 1,000 V, producing current pulses of 40-100 ns duration. The pulses consumed between 168 μJ and 6 mJ each.

A planar version of this device was also reported [9]. It consisted of a circular anode and three semi-spherical cathodes (spaced 50 μm apart and 300 μm in width). The electrode structures were 1 μm-thick Ti patterned on a glass substrate. Typical sensitivities were 9800 ppm/Torr in lower pressures (from 30-100 Torr) and 1400 ppm/Torr in higher pressures (from 100-200 Torr).

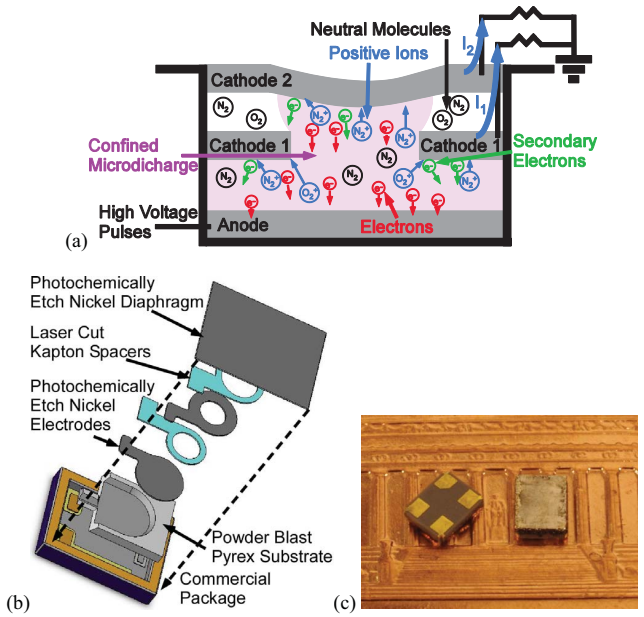

Fig. 6. Pressure sensor device concept. (a) Diagram of a microdischarge between a single anode and two cathodes. (b) Component integration illustrating stacked electrode/spacer structure within a commercial package before diaphragm attachment. (c) Photograph of pressure sensors in commercial Kyocera ceramic packages with laser-welded diaphragms on a penny [65].

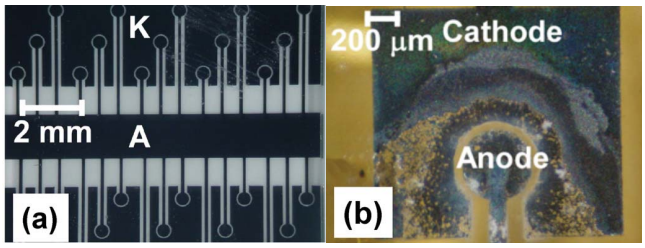

Fig. 7. (a) Micro-SIP device that utilizes thin-film titanium electrodes patterned on glass substrate and comprises a single anode and two cathodes. Each cathode has 15 discharge gaps and encompasses an area of 33 mm^2. (b) Micro-SIP electrodes displaying remains of a cathode after reactive sputtering, illustrating areas of complete titanium sputtering [15], [72].

In the examples described above, the sensors were intended to monitor pressures inside clean, dust-free environments e.g., vacuum systems, which eased certain chip-level packaging considerations. However, the monitoring of harsh environments in the presence of fluid ambient requires additional features. In the case of oil exploration, the sensor is required to operate under pressures of several atms, while surrounded by a mixture of petroleum, water, and gas. A configuration that allows the discharge cavity to be sealed and isolated from the environment is necessary.

Miniaturized microdischarge-based pressure sensors sealed within ceramic packages were reported [65]. The sensor configuration consisted of an anode and a stationary cathode that were encapsulated within the package. The lid of the package was a deflecting diaphragm that responded to externally applied pressure, and also served as the competing cathode (Fig. 6a). As the distance between the anode and the deflected diaphragm decreased, the fraction of current flowing through it increased, at the cost of the current through the stationary cathode. The assembly and final structure of this device are illustrated in Fig. 6b and Fig. 6c, respectively. The housing was a ceramic package with external dimensions of $2.05 \times 1.65 \times 0.5$ mm^3(Kyocera, Japan). The active volume of these devices was 0.057 mm^3, which was $\approx 10\times$ smaller than previously reported microdischarge-based vacuum sensors, whereas the pressure range was $\approx 6\times$ higher. This particular sensor was able to measure pressure up to 15 atm. and provided a sensitivity of 2,864 ppm/psi (42,113 ppm/atm.).

IV. On-Chip Pressure Regulation and Contaminant Gas Removal Using Microdischarges

As feature sizes and device volumes in micro-scale sensors and actuators are scaled down, the generation and maintenance of vacuum levels in sealed micro-cavities becomes increasingly difficult. The internal pressure can be easily increased by even small amounts of parasitic leakage, such as outgassing from surfaces or diffusion of gases through the cavity walls. Removal of moisture and less reactive gases such as nitrogen can be particularly challenging. The absorption or removal of gas from these sealed cavities can be used to lower the pressure below the initial sealing pressure or to maintain a desired pressure over extended time periods.

Pressure regulation methods that do not depend on moving parts and can be easily integrated are the most desirable. Nonevaporable getters (NEG), thin-film getters (e.g., Nanogetters), and reactive sealing approaches [66-68] have been widely reported. While these technologies have worked on both the macroscopic and microscopic scales, these typically operate in the mTorr range and require activation temperatures of 200-550°C. For example, ST707, an alloy of Zr-V-Fe, requires activation at 450-500°C [69]. Micromachined thermal molecular pumps, which are also without moving parts, have been proposed - Knudsen pumps [70, 71] belong in this category. However, these can typically require higher operating temperatures and power than is desirable for certain applications. For devices that require pressure control at lower operating temperatures (typically 100-150°C), alternative or complementary means of controlling the pressure are needed.

Micro-scale discharges between thin-film titanium electrodes on a microchip have been used to chemisorb oxygen and nitrogen through reactive sputtering of the cathode [15, 72]. The device structure had a total footprint of 1 cm^2 with a total cathode area of 33 mm^2 (Fig. 7a). Using DC discharges, the device was reported to remove 168 Torr of air from a cavity volume of 6.33 cm^3 (Fig. 8). Starting at 200 Torr, the removal rate of air was 7.2 Torr/h; for oxygen it was 11.5 Torr/h, and nitrogen 3.4 Torr/h. The relative humidity was reduced 6%/h, starting with 61%. A $5\times$ increase in pump power efficiency was obtained through the use of 25 ms pulsed discharges compared to DC discharges. After extended discharge operation, the cathode areas of the titanium were sputtered uniformly around its perimeter and almost completely removed down to the glass substrate (Fig. 7b). The anode remained largely intact.

Micro-SIPs can also be used for the purification of gas samples. In particular, microdischarges have been used to purify

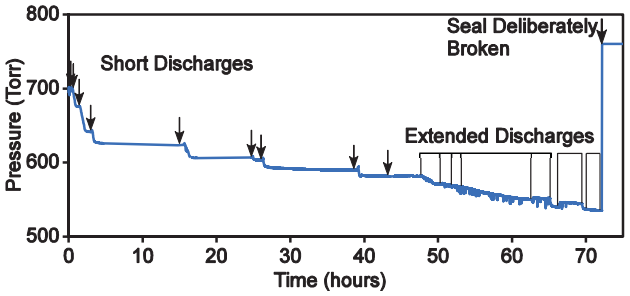

Fig. 8. Pressure drop in a 6.33-cm^3 package over time. Fifteen consecutive discharges drop the pressure 168 Torr. The pressure remains stable over periods of 10 h of micro-SIP inactivity and returns to atmospheric pressure when the package is opened [15], [72].

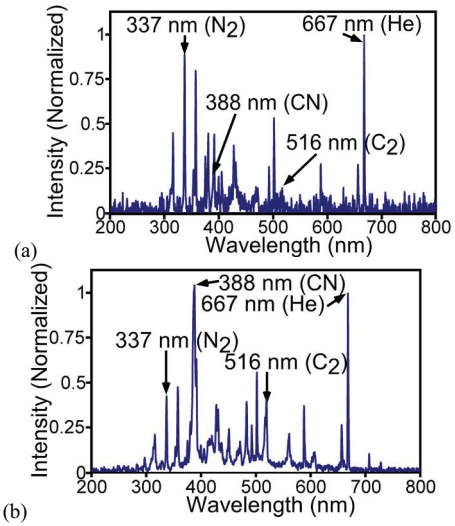

Fig. 9. Impurity removal. (a) Spectra of acetone sample (normalized to helium at 667.8 nm) backfilled with helium during gas purification at 200 °C. Spectrum recorded before purification, showing strong nitrogen emissions and low C_2 emissions. (b) Spectrum recorded after purification, showing diminished nitrogen and increased CN and C_2 emissions [73].

both organic and inorganic gas mixtures for spectral detection of chemicals [73]. The device used an electrode pattern with circular discharge gaps (of 50 μm) for uniform sputtering and relatively large cathode areas (1.52 mm^2) to increase the available titanium. There were three anode/cathode pairs per chip and the entire device had an area of 25 mm^2. For this particular work, a microdischarge-based optical emission sensor (with a 100 μm discharge gap and 25 mm^2 device area) was used to monitor the purification process. (This sensor was able to detect carbon in acetone vapor at concentrations as low as 17 ppm in an air ambient without any preconcentration.) The purification device and optical emission sensor were enclosed in a re-sealable package with a cavity volume of 4 cm^3. To determine the level of purification, the ratio of intensities of the strongest carbon emission line (C_2, 516.4 nm) to the strongest nitrogen emission line (N_2, 337.1 nm) was measured. The device increased the detectability of carbon from an acetone sample by a factor of 8× (Fig. 9). In a separate set of experiments, the purification of inorganic gas mixtures was also demonstrated; in a mixture that contained helium (99.25%) and air (0.75%), a 56.5× reduction in nitrogen and 16.2× reduction in oxygen were typically achieved. The final concentrations of these contaminant gases were 90 ppm and 70 ppm, respectively. The nitrogen concentration typically fell by 75% within 30 minutes.

V. Radiation Detection

At the macro-scale, radiation detectors based on electrical discharges in gaseous media (e.g., Geiger counters) are often favored for field use [74]. Known to be robust and relatively simple to use, these devices can operate over a large temperature range and measure a wide range of radiation species and energies. Typically, gas-based radiation detectors utilize a gas volume with an applied electric field. Ionizing radiation (e.g., a beta-particle) interacts with the gas and creates charged particles. These particles are accelerated by the electric field, leading to electron multiplication (and depending on the degree of the field, in certain cases an avalanche breakdown) that produces a current pulse. One of the advantages of operating at higher electric fields (e.g., in the Geiger-Mueller region) is the large inherent signal amplification that occurs via electron multiplication. This reduces the burden of additional electronics such as amplifiers and pulse-shaping circuits.

Gas-based detectors can be used to detect most radiation species. As noted above, beta-particles interact directly with the gas, which trigger current pulses. In contrast, gamma radiation or high-energy photons are converted into photoelectrons by interaction with high-density metals that are used for the electrodes and for the walls encapsulating the fill-gas [75-78]. Gamma radiation interacts with materials primarily by three collision processes, i.e., the photoelectric effect, Compton scattering, and pair production. The energy of the incoming photon determines the collision process. Collisions involving low energy photons are dominated by the photoelectric effect, where the impinging photon transfers all of its energy to an ejected photoelectron. Collisions of higher energy photons (up to 1.022 MeV) cause Compton scattering, in which a photoelectron and a secondary photon are emitted. For incident photons with higher energy, the collision process is dominated by pair production, where a high-energy electron and positron are ejected. The positron is quickly annihilated by a free electron, resulting in the emission of two photons with identical energies of 0.51 MeV. The use of high-pressure fill-gases with large atomic numbers [79, 80] can also increase the interaction probability.

Gas-based detectors can be adapted for neutrons by incorporating nuclides with large neutron cross-sections (e.g., ^{3}He, ^{10}B, and ^{235}U) in high-pressure (1-10 atmosphere) environments [74, 81, 82]. These nuclides react with the neutrons to create charged particles (e.g., protons and alpha-particles), which can trigger electron avalanches in the fill-gas. The major source of background noise is high-energy photons, which can register similar energies and are difficult to differentiate from the neutrons.

Gas-based radiation detectors with sub-millimeter feature sizes have been explored for several decades. In the late 1960's, Charpak reported position localization of charged particles using gas avalanche detectors with an array of

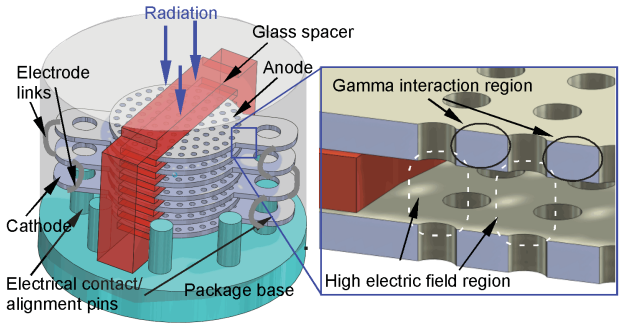

Fig. 10. Radiation detector concept. The detector comprises a stacked arrangement of multielectrode stainless steel elements (i.e., anode and cathode) and a glass insulator, assembled within a commercial TO-5 package base. Each electrode is an array of three or four "linked" elements. Machined shelves in the spacer maintain a 200-μm-wide interelectrode spacing between each electrode layer. Gamma radiation interacts with the metal layers, which releases photoelectrons into the biased gap. These charged particles trigger an avalanche within the biased gap, leading to wireless signaling [17].

very thin, closely-spaced wire electrodes [83]. The multiwire proportional chamber (MWPC) was able to achieve submillimeter accuracies over detection areas exceeding a square meter, with fast recovery times and very high count rates.

Advances in lithographic manufacturing have played a key role in improving the capability and performance of microfabricated gas-based radiation detectors. Planar configurations have provided an increase in structural stability, as well as greater uniformity in detector performance. At the cost of signal amplification, these configurations tend to operate in a lower field region, to avoid spurious discharges that can potentially damage the electrode structures. One of the first micropatterned detectors used a microstrip electrode structure (MSGC) with alternating thin metal strips for the anode and cathode (typically, 10 μm and 100 μm, respectively) laid on an insulating support [84, 85]. Since then, several other detector structures have been reported including the MICROMEGAS [86]. This used a small-gap (50-100 μm-wide), parallel-plate design where the radiation-induced electrons were pulled through a dense wire micromesh structure (cathode) located between the plates, leading to signal multiplication and finally collection at the anode strip. The micro-CAT [87] used a metal electrode plane (cathode) with a fine mesh grid of machined holes. Localized electron multiplication occurred through the hole structure and the resulting electrons were accelerated toward an anode plane. It was coupled to a 2D resistive readout system. The gas electron multiplier (GEM) [88] was essentially a thin insulating film (50-100 μm-thick polyimde) with a thin metal laminate (1-5 μm-thick) on both sides. The structures were perforated, with openings 25-150 μm in diameter spaced apart by 50-200 μm [88, 89]. Similar to the micro-CAT, the electrons were pulled through the holes by the electric field and collected by a 2D resistive readout system. These devices focused on achieving high spatial resolution and were targeted for position sensing applications, such as medical imaging and nuclear particle tracking [88, 90].

One inherent limitation of miniature detectors is that the reduction of size results in low detection efficiencies (1-3%), in particular for gamma and neutron radiation [74, 91]. Utilizing multiple stacks of a detector structure can potentially increase detection efficiencies for a device with a given form factor. Past work on stacking detector structures in order to achieve improved performance included a variation on the GEM [89]. The triple GEM detector utilized the parallel stacking of three GEM structures in order to increase the amplification of the carriers (or gain) at lower bias conditions (as compared to a single GEM). These GEM stacked structures required several bias voltages (for each layer of GEM, as well as for the drift and readout plate) for proper operation.

A scalable path for increasing detection efficiency has been recently reported [17]. This approach improved the overall effective sensitive volume for a given detector by utilizing a 3D stack of electrodes, increasing the amount of high-Z material for gamma interaction, and utilizing the entire volume of a given package - in this effort a TO-5 header. Only one electrical bias was utilized. This structure built upon a previous effort in which a single anode-cathode pair was reported [16].

The stacked detector structure included two sets of perforated, stainless steel electrode arrays that were microfabricated from metal foil (Fig. 10). The anode array had 4 elements, whereas the cathode array had 3 elements. The elements in each set were connected by V-shaped links. Each set was designed to be plastically deformed into a stack of parallel elements. These elements were inserted into an insulating glass structure with micromachined shelves, which maintained a 200 μm-wide anode-cathode interelectrode spacing. The glass structure and steel elements were installed onto the base of a TO-5 package using the package pins for stability and electrical access.

In operation, this device has a high electric field (e.g., 4-5 MV/m with a bias of 600V) near the electrode perforations and a lower field (e.g., 2-2.5 MV/m) away from these. The lower field region was used to guide the generated photoelectrons towards the higher field region, which promoted avalanching or multiplication of the photoelectrons.

Direct wireline measurements of the count rate were provided by a high-frequency inductive current probe attached to an oscilloscope (Agilent DSO8064A, 600 MHz). The applied biases for the detector ranged from 500-575 V for an Ar fill-gas operating near 760 Torr. Typical current discharge pulses were of 25-50 ns duration and 100 mA amplitudes (Fig. 11a). For a radiation source such as 99 μCi ^{137}Cs, typical count rates were near 127-170 counts per minute (cpm) at a distance of 30.5 cm. Measured background rates (in the absence of a radiation source) ranged from 1.1-5.8 cpm. The intrinsic detector efficiency, ε_{int}, is defined as the percentage of radiation incident on the detector that results in recorded pulses [74]. Assuming predominantly gamma detection, the intrinsic detection efficiency was $\approx$4%.

The receiver operating characteristic (ROC) curve, which is used for a variety of sensors, depicts the compromise between successful detection and false positives [74, 92, 93]. The true positive rate (TPR) is the fraction of true detection events (i.e., when a source is present) above a predetermined threshold of counts. The false positive rate (FPR) is the fraction of detection events above the same threshold without a source present, i.e.,

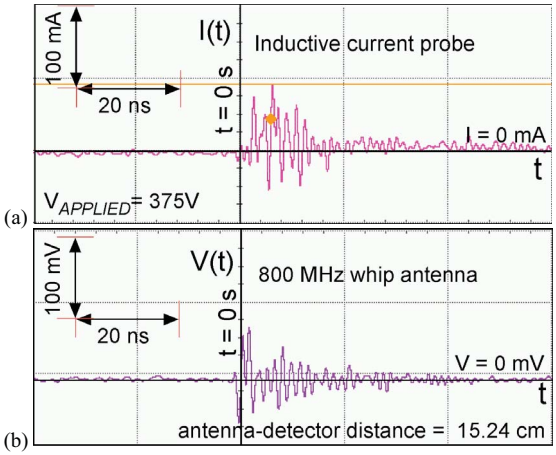

Fig. 11. Discharge-induced radio transmission. (a) Current pulse measurement (of a "count") showing approximately 100-mA peaks and 20–50-ns duration. (b) Transmitted wireless signal was received using an 800-MHz whip antenna attached to an oscilloscope. The antenna–detector distance was 15.24 cm. The time domain behavior of the RF transmission followed closely with the current pulse measurement. 99 μCi from ^{137}Cs was used [17].

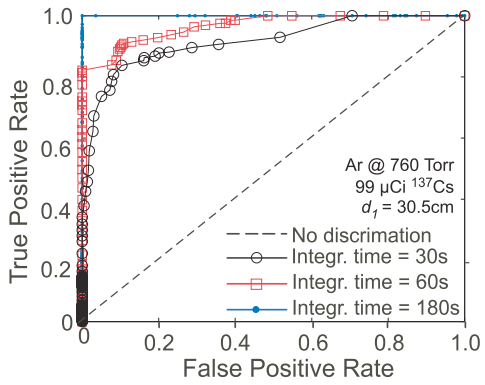

Fig. 12. Receiver operating characteristics. The ROC curves for various integration times ranging from 30 to 180 s. The average count rate and background rate were about 78 and 5.76 cpm, respectively [17].

background events. Integration time is the measurement time window during which the device is collecting detection events or "counts". For superior performance, the TPR must approach 1 at a low value of FPR. As detectors are miniaturized, the ratio of TPR to FPR is expected to drop, because the radiation from a target sample may simply miss the detector, or pass through it without interaction. Data show that an increase in the signal integration time can compensate for this. The ROC curves obtained for the detectors described in [17] are shown in Fig. 12. These were measured with a bias of 520 V, and source-detector distance of 30.5 cm. An integration time of 180 s resulted in an ROC curve approaching the ideal ROC curve (FPR = 0, TPR = 1). As integration times increased from 30 s to 180 s, the likelihood of a true detection event increased from 80% to near 100% for a corresponding false positive rate near zero.

There is interest in miniature, radiation detector microsystems for environmental monitoring and homeland security applications. Individually, microfabricated radiation detectors could be used in applications for which the weight or space is at a premium, e.g., micro-air-vehicles (MAVs). As elements of a network, the detectors may facilitate reconfigurable deployment in public spaces (e.g., football stadiums, amusement parks, and shopping malls), or in dangerous and inaccessible environments (e.g., contaminated or remote areas) [94, 95]. In these contexts, wireless signaling capability can be a useful feature.

Under appropriate conditions, microdischarges can concomitantly produce a wireless signal. Gas-based discharges were employed for wireless communication in the mid-1890's using Marconi's spark gap transmitters [96]. The discharge gaps were relatively large (on the order of cm's), achieving transmission distances on the order of kilometers. In 1901, Bose utilized these discharges within waveguides to generate microwaves. More activity on this topic has been reported [97]. It has been shown that even micro-scale discharges can be used for wireless signaling [16, 17, 98].

The gamma detectors reported in [16, 17] demonstrated wideband wireless transmission capability. The devices were operated in an argon fill-gas near atmospheric pressure. The generated frequency spectra had been measured to extend from the low kHz to the GHz. A typical transmitted wireless spectra received using a commercial 800 MHz whip antenna is shown in Fig. 11b. The shape and duration were similar in behavior to the measured current pulses. The antenna was 30.5 cm in length and positioned at an antenna-detector distance of 15.24 cm, perpendicular to the ground. The receiving antenna was able to receive transmitted pulses at a rate similar to the wireline count rates. The received signal attenuated with increasing antenna-detector distance. A similar device that was previously reported by the same team used a fill-gas containing air and neon, and operated near atmospheric pressure [98, 99]. The resulting microdischarge transmitted a wideband electromagnetic signal that was detected using commercial AM/FM receivers.

VI. Conclusion

The examples described in the preceding sections provide an indication of the diverse applications that can be envisioned for sensors based on microdischarges. The potential benefits of microdischarges include direct electrical or electro-optical transduction, as in the chemical sensors that use emission spectroscopy; the ability to operate under harsh environmental conditions, as in the stacked bulk metal foil pressure sensors; the ability to provide pressure regulation and in addition, gas contaminant removal, as in the micro-SIPs; and the ability for wireless radio frequency signaling, as in the radiation detectors. These examples also illustrate the possibility of lithographic manufacturing methods that can be exploited for high volume commercial production. The choice of materials, in particular, electrode materials, will affect not only the performance of the sensors but also device longevity. The encapsulation and packaging of microdischarge-based sensors can leverage existing commercial approaches.

The high promise of microdischarge-based sensors is accompanied by a number of research challenges. The ability to control various physical aspects of the microdischarge, e.g., the ionization level, the energy, and the spatial and temporal

extent of microdischarges are important goals. Multi-electrode structures, dynamic biasing schemes, and other such methods, some of which have been discussed in this paper, may offer a path forward. Further insight into the mechanisms governing the wireless transmissions by microdischarges will help to expand the field of discharge-based applications. Predictive modeling that covers time-, spatial-, and frequency-domains is essential to spur further the application of microdischarges. As our understanding evolves on these fronts, new devices and applications are certain to emerge.

ACKNOWLEDGMENT

The authors would like to thank X. Luo, M. Anderson, R. Arslanbekov, R. Gharpurey, V. Kolobov, B. Mitra, L. Que, R. Selvaganapathy, A. Wendt, C. Wilson, S. Wright, and M. Zorn, and others who have collaborated on various parts of the effort over the years.

REFERENCES

[1] J. G. Eden and S. J. Park, "Microcavity plasma devices and arrays: A new realm of plasma physics and photonic applications," *Plasma Phys. Controlled Fusion*, vol. 47, pp. 83–92, Nov. 2005.

[2] R. Foest, M. Schmidt, and K. Becker, "Microplasmas, an emerging field of low-temperature plasma science and technology," *Int. J. Mass Spectro.*, vol. 248, no. 3, pp. 87–102, Feb. 2006.

[3] S. Wright, "Microdischarge-based pressure controlling devices and their applications to chemical sensing in harsh environments," Ph.D. dissertation, Dept. Electr. Eng. Comput. Sci., Univ. Michigan, MI, 2008.

[4] M. Kushner, "Modelling of microdischarge devices: Plasma and gas dynamics," *J. Phys. D Appl. Phys.*, vol. 38, no. 11, pp. 1633–43, Jun. 2005.

[5] J. Choi, F. Iza, J. K. Lee, and C. Ryu, "Electron and ion kinetics in a DC microplasma at atmostpheric pressure," *Trans. Plasma Sci.*, vol. 35, no. 5, pp. 1274–1278, Oct. 2007.

[6] K. H. Becker, K. H. Schoenbach, and J. G. Eden, "Microplasmas and applications," *J. Phys. D: Appl. Phys.*, vol. 39, pp. 55–70, Jan. 2006.

[7] C. Wilson, Y. Gianchandani, and A. Wendt, "High-voltage constraints for vacuum packaged microstructures," *J. Microelectromech. Syst.*, vol. 12, no. 6, pp. 835–839, Dec. 2003.

[8] C. G. Wilson, Y. B. Gianchandani, R. Arslanbekov, V. Kolobov, and A. Wendt, "Profiling and modeling of DC nitrogen microplasmas," *J. Appl. Phys.*, vol. 94, no. 5, pp. 2845–2851, Sep. 2003.

[9] S. A. Wright and Y. B. Gianchandani, "Discharge-based pressure sensors for high-temperature applications using 3-D and planar microstructures," *J. Microelectromech. Syst.*, vol. 18, no. 3, pp. 736–743, Jun. 2009.

[10] K. M. Welch, "Major advances in capture pumps in the last 50 years," *J. Vacuum Sci. Technol. Vacuum Surfaces Films*, vol. 21, no. 5, pp. 19–24, Sep. 2003.

[11] L. Holland, "Theory and design of getter-ion pumps," *J. Scientific Instrum.*, vol. 36, no. 3, pp. 105–116, Mar. 1959.

[12] D. M. Mattox, "Reactive sputter deposition," *Plating Surface Finish.*, vol. 88, no. 1, pp. 74–77, Jan. 2001.

[13] D. R. Denison, "Performance of a new electrostatic getter-ion pump," *J. Vacuum Sci. Technol.*, vol. 4, no. 4, pp. 156–162, Jul. 1967.

[14] B. F. Coll and M. Chhowalla, "Modelization of reaction kinetics of nitrogen and titanium during TiN arc deposition," *Surface Coatings Technol.*, vols. 68–69, pp. 131–140, Dec. 1994.

[15] S. Wright and Y. Gianchandani, "Controlling pressure in microsystem packages by on-chip microdischarges between thin-film titanium electrodes," *J. Vacuum Sci. Technol. B*, vol. 25, no. 5, pp. 1711–1720, 2007.

[16] C. K. Eun and Y. B. Gianchandani, "A microfabricated steel and glass radiation detector with inherent wireless signaling," *J. Micromech. Microeng.*, vol. 21, no. 1, pp. 015003-1–015003-11, 2011.

[17] C. K. Eun and Y. B. Gianchandani, "A wireless-enabled microdischarge-based radiation detector utilizing stacked electrode arrays for enhanced detection efficiency," *J. Microelectromech. Syst.*, vol. 20, no. 3, pp. 636–643, Jun. 2011.

[18] V. Karanassios, "Microplasmas for chemical analysis: Analytical tools or research toys?" *Spectrochim. Acta B Atomic Spectro.*, vol. 59, no. 7, pp. 909–928, Jul. 2004.

[19] M. Miclea and J. Franzke, "Analytical detectors based on microplasma spectrometry," *Plasma Chem. Plasma Process.*, vol. 27, no. 2, pp. 205–24, Apr. 2007.

[20] M. Miclea, M. Okruss, K. Kunze, N. Ahlman, and J. Franzke, "Microplasma-based atomic emission detectors for gas chromatography," *Analytical Bioanalytical Chem.*, vol. 388, no. 8, pp. 1565–1572, Aug. 2007.

[21] A. Michels, S. Tombrink, W. Vautz, M. Miclea, and J. Franzke, "Spectroscopic characterization of a microplasma used as ionization source for ion mobility spectrometry," *Spectrochim. Acta Part B Atomic Spectro.*, vol. 62, no. 11, pp. 1208–1215, Nov. 2007.

[22] J. Broekaert, "The development of microplasmas for spectrochemical analysis," *Analytical Bioanalytical Chem.*, vol. 374, no. 2, pp. 182–187, 2002.

[23] J. Broekaert, V. Siemens, and N. H. Bings, "Microstrip microwave induced plasma on a chip for atomic emission spectral analysis," *IEEE Trans. Plasma Sci.*, vol. 33, no. 2, pp. 560–561, Apr. 2005.

[24] J. Franzke, K. Kunze, M. Milcea, and K. Niemax, "The dielectric barrier discharge as a detector for gas chromatography," *Spectrochim. Acta Part B Atomic Spectros.*, vol. 58, no. 8, pp. 1435–1443, Aug. 2003.

[25] J. Franzke and M. Miclea, "Sample analysis with miniaturized plasmas," *Appl. Spectros.*, vol. 60, no. 3, pp. 80–90, Mar. 2006.

[26] Y. G. Gianchandani, S. A. Wright, C. K. Eun, C. G. Wilson, and B. Mitra, "Exploring microdischarges for portable sensing applications," *Analytical Bioanalytical Chem.*, vol. 395, no. 3, pp. 559–575, 2009.

[27] B. Mitra, B. Levey, and Y. Gianchandani, "Hybrid arc/glow microdischarges at atmospheric pressure and their use in portable systems for liquid and gas sensing," *IEEE Trans. Plasma Sci.*, vol. 36, no. 4, pp. 1913–1924, Aug. 2008.

[28] R. Braman and A. Dynako, "Direct current discharge spectral emission-type detector," *Analytical Chem.*, vol. 40, no. 1, pp. 95–106, Jan. 1968.

[29] G. Lambertus, A. Elstro, K. Sensenig, J. Potkay, M. Agah, S. Scheuering, K. Wise, F. Dorman, and R. Sacks, "Design, fabrication, and evaluation of microfabricated columns for gas chromatography," *Analytical Chem.*, vol. 76, no. 9, pp. 2629–2637, May 2004.

[30] M. Agah, G. Lambertus, R. Sacks, and K. Wise, "High-speed MEMS-based gas chromatography," *J. Microelectromech. Syst.*, vol. 15, no. 5, pp. 1371–1378, Oct. 2006.

[31] C. Brede, E. Lundanes, T. Greibrokk, and S. Pedersen-Bjergaard, "Capillary gas chromatography coupled with negative ionization microplasma mass spectrometry for halogen-selective detection," *J. analytical Atomic Spectro.*, vol. 15, no. 1, pp. 55–60, 2000.

[32] J. Eijkel, H. Stoeri, and A. Manz, "Molecular emission detector on a chip employing a direct current microplasma," *Analytical Chem.*, vol. 71, no. 14, pp. 2600–2606, Jul. 1999.

[33] J. Eijkel, H. Stoeri, and A. Manz, "Atmospheric pressure dc glow discharge on a microchip and its application as a molecular emission detector," *J. Analytical Atomic spectro.*, vol. 15, no. 3, pp. 297–300, 2000.

[34] J. Eijkel, H. Stoeri, and A. Manz, "Dc microplasma on a chip employed as an optical emission detector for gas chromatography," *Analytical Chem.*, vol. 72, no. 11, pp. 2547–2552, Jun. 2000.

[35] F. Bessoth, O. Naji, J. Eijkel, and A. Manz, "Toward an on-chip gas chromatograph: The development of a gas injector and a dc plasma emission detector," *J. Analytical Atomic Spectro.*, vol. 17, no. 8, pp. 794–799, Aug. 2002.

[36] O. Naji and A. Manz, "A double plasma gas chromatography injector and detector," *Lab Chip*, vol. 4, no. 5, pp. 431–437, 2004.

[37] X. Luo, W. Zhu, B. Mitra, J. Liu, T. Liu, X. Fan, and Y. B. Gianchandani, "A chemical detector for gas chromatography using pulsed discharge emission spectroscopy on a microchip," in *Proc. Amer. Geophys. Union Fall Meeting*, San Francisco, CA, Dec. 2011.

[38] R. W. B. Pearse, *The Identification of Molecular Spectra*, 3rd ed. London, U.K.: Chapman & Hall, 1963.

[39] B. Mitra and Y. B. Gianchandani, "The detection of chemical vapors in air using optical emission spectroscopy of pulsed microdischarges from two and three electrode microstructures," *IEEE Sens. J.*, vol. 8, no. 8, pp. 1445–1454, Aug. 2008.

[40] J. Yoon, D. Lee, H. Nam, G. Cha, T. Strong, and R. Brown, "Ion sensors using one-component room temperature vulcanized silicone rubber matrices," *J. Electroanalytical Chem.*, vol. 464, no. 2, pp. 135–142, Mar. 1999.

[41] S. Taylor, B. Srigengan, J. Gibson, D. Tindall, R. Syms, T. Tate, and M. Ahmad, "Miniature mass spectrometer for chemical and biological sensing," *Proc. SPIE*, vol. 4036, pp. 187–193, Apr. 2000.

[42] R. Miller, E. Nazarov, G. Eiceman, and A. King, "A MEMS radio-frequency ion mobility spectrometer for chemical vapor detection," *Sens. Actuat. A Phys.*, vol. A91, no. 3, pp. 301–312, Jul. 2001.

[43] G. Jenkins and A. Manz, "A miniaturized glow discharge applied for optical emission detection in aqueous analytes," *J. Micromech. Microeng.*, vol. 12, no. 5, pp. 19–22, Sep. 2002.

[44] T. Cserfalvi and P. Mezei, "Subnanogram sensitive multimetal detector with atmospheric electrolyte cathode glow discharge," *J. Analytical Atomic Spectro.*, vol. 18, no. 6, pp. 596–602, Jun. 2003.

[45] H. Kim, J. Lee, M. Kim, T. Cserfalvi, and P. Mezei, "Development of open-air type electrolyte-as-cathode glow discharge-atomic emission spectrometry for determination of trace metals in water," *Spectrochim. Acta Part B*, vol. 55, no. 7, pp. 823–831, Jul. 2000.

[46] K. Johnson, W. Wilp, and V. Karanassios, "Micro-fluidics in environmental monitoring: Liquid micro-samples by an in-torch vaporization micro-plasma device ITV-MPD," *Proc. SPIE*, vol. 4205, pp. 347–352, Feb. 2001.

[47] V. Karanassios, K. Johnson, and A. Smith, "Micromachined, planar-geometry, atmospheric-pressure, battery-operated microplasma devices (MPDs) on chips for analysis of microsamples of liquids, solids, or gases by optical-emission spectrometry," *Analytical Bioanalytical Chem.*, vol. 388, no. 8, pp. 1595–1604, Aug. 2007.

[48] W. Davis and R. Marcus, "An atmospheric pressure glow discharge optical emission source for the direct sampling of liquid media," *J. Analytical Atomic Spectro.*, vol. 16, no. 9, pp. 931–937, Sep. 2001.

[49] R. Marcus and W. Davis, "An atmospheric pressure glow discharge optical emission source for the direct sampling of liquid media," *Analytical Chem.*, vol. 73, no. 13, pp. 2903–2910, Jul. 2001.

[50] C. Wilson and Y. Gianchandani, "Spectral detection of metal contaminants in water using an on-chip microglow discharge," *IEEE Trans. Electron Dev.*, vol. 49, no. 12, pp. 2317–2322, Dec. 2002.

[51] L. Que, C. Wilson, and Y. Gianchandani, "Microfluidic electrodischarge devices with integrated dispersion optics for spectral analysis of water impurities," *J. Microelectromech. Syst.*, vol. 14, no. 2, pp. 185–191, Apr. 2005.

[52] M. Zorn, C. Wilson, Y. B. Gianchandani, and M. Anderson, "Detection of aqueous metals using a microglow discharge atomic emission sensor," *IEEE Sens. Lett.*, vol. 2, no. 3, pp. 179–185, Sep. 2004.

[53] B. Mitra, C. Wilson, L. Que, P. Selvaganapathy, and Y. Gianchandani, "Microfluidic discharge-based optical sources for detection of biochemical," *Lab Chip*, vol. 6, no. 1, pp. 60–65, 2006.

[54] B. Mitra, "DC pulsed-powered microdischarges on planar electrodes and their use in vapor and liquid phase chemical sensing in ambient air," Ph.D. dissertation, Dept. Electr. Eng. Comput. Sci., Univ. Michigan, MI, 2008.

[55] R. P. Haugland, "Handbook of fluorescence probes and research chemicals: Molecular probes," *Biochem. Educat.*, vol. 22, no. 2, pp. 1–83, 1996.

[56] R. Fielder, K. Stingson-Bagby, and M. Palmer, "Harsh-environment fiber optic sensors for structural monitoring applications," *Proc. SPIE*, vol. 5388, no. 1, pp. 399–409, 2004.

[57] D. Abeysinghe, S. Dasgupta, H. Jackson, and J. Boyd, "Novel MEMS pressure and temperature sensors fabricated on optical fibers," *J. Micromech. Microeng.*, vol. 12, no. 3, pp. 229–235, May 2002.

[58] Y. Zhao, Y. Liao, and S. Lai, "Simultaneous measurement of down-hole high pressure and temperature with a bulk-modulus and FBG sensor," *IEEE Photon. Technol. Lett.*, vol. 14, no. 11, pp. 1584–1586, Nov. 2002.

[59] C. Li, J. Huang, R. Lin, D. Lii, and C. Chen, "Performance characterization of nonevaporable porous Ti getter films," *J. Vacuum Sci. Technol.*, vol. 25, no. 5, pp. 1373–1380, Sep. 2007.

[60] S. Guo, H. Eriksen, K. Childress, A. Fink, and M. Hoffman, "High temperature smart-cut SOI pressure sensor," *Sens. Actuat. A: Phys.*, vol. 154, no. 2, pp. 255–260, Sep. 2009.

[61] A. Ned, R. Okojie, and A. Kurtz, "6H-SiC pressure sensor operation at 600 °C," in *Proc. 4th Int. High Temperature Electron. Conf.*, Albuquerque, NM, 1998, pp. 257–60.

[62] S. Fricke, A. Friedberg, T. Ziemann, E. Rose, G. Muller, D. Telitschkin, S. Ziegenhagen, H. Seidel, and U. Schmidt, "High temperature (800 °C) MEMS pressure sensor development including reusable packaging for rocket engine applications," in *Proc. MNT Aerospace Applicat.*, 2006, pp. 287–291.

[63] C. Edelmann, "Measurement of high pressures in the vacuum range with the help of hot filament ionization gauges," *Vacuum*, vol. 41, nos. 7–9, pp. 2006–2008, 1990.

[64] D. Allen, "The state of the art of photochemical machining at the start of the twenty-first century," in *Proc. Institution Mech. Eng. Part B: J. Eng. Manufact.*, vol. 217, no. 5, pp. 643–650, 2003,

[65] S. A. Wright, H. Z. Harvey, and Y. Gianchandani, "A microdischarge-based deflecting-cathode pressure sensor in a ceramic package," *J. Microelectromech. Syst.*, to be published.

[66] H. J. Halama and Y. Guo, "Nonevaporable getter investigation at the national synchrotron light source," *J. Vacuum Sci. Technol. A*, vol. 9, no. 3, pp. 2070–2073, May–Jun. 1991.

[67] H. Henmi, S. Shoji, Y. Shoji, K. Yoshimi, and M. Esashi, "Vacuum packaging for microsensors by glass-silicon anodic bonding," *Sens. Actuat. A: Phys.*, vol. 43, nos. 1–3, pp. 243–248, May 1994.

[68] D. R. Sparks, S. Massoud-Ansari, and N. Najafi, "Chip-level vacuum packaging of micromachines using nanogetters," *IEEE Trans. Adv. Packag.*, vol. 26, no. 3, pp. 277–282, Aug. 2003.

[69] *St707 Getter Alloy for Vacuum Thermal Insulation* [Online]. Available: http://www.saesgetters.com/default.aspx?idpage=273

[70] J. Hobson and D. Salzman, "Review of pumping by thermal molecular pressure," *J. Vacuum Sci. Technol. A: Vacuum Surfaces Films*, vol. 18, no. 4, pp. 1758–1765, Jul. 2000.

[71] S. McNamara and Y. B. Gianchandani, "On-chip vacuum generated by a micromachined Knudsen pump," *J. Microelectromech. Syst.*, vol. 14, no. 4, pp. 741–746, Aug. 2005.

[72] S. A. Wright and Y. B. Gianchandani, "A harsh environment, multi-plasma microsystem with pressure sensor, gas purifier, and chemical detector," in *Proc. IEEE Int. Conf. Micro Electro Mech. Syst.*, Kobe, Japan, Jan. 2007, pp. 115–118.

[73] S. A. Wright and Y. B. Gianchandani, "Contaminant gas removal using thin-film Ti electrode microdischarges," *Appl. Phys. Lett.*, vol. 95, no. 11, pp. 111504-1–111504-3, Sep. 2009.

[74] G. F. Knoll, *Radiation Detection and Measurement*. New York: Wiley, 2000.

[75] B. Shafrir and A. Seidman, "High efficiency gamma-ray metal converters," *Nuclear Instrum. Methods*, vol. 129, no. 1, pp. 177–186, 1975.

[76] U. Shimoni, B. Sheinfux, A. Seidman, J. Grinberg, and Z. Avrahami, "Investigations on metal converters for gamma-ray detection and mapping," *Nuclear Instrum. Methods*, vol. 117, no. 2, pp. 599–603, 1974.

[77] M. Nakamura, "The energy spectra and the quantum efficiencies of electrons emitted from the metallic elements irradiated by 60Co gamma-rays," *J. Appl. Phys.*, vol. 54, no. 6, pp. 3141–3149, Jun. 1983.

[78] J. Hirschfelder, J. Magee, and M. Hull, "The penetration of gamma-radiation through thick layers. I. Plane geometry, Klein–Nishina scattering," *Phys. Rev.*, vol. 73, no. 8, pp. 852–862, Apr. 1948.

[79] C. E. Lehner, Z. He, and G. F. Knoll, "Intelligent gamma-ray spectroscopy using 3-D position-sensitive detectors," *IEEE Trans. Nuclear Sci.*, vol. 50, no. 4, pp. 1090–1097, Aug. 2003.

[80] S. D. Kiff, Z. He, and G. C. Tepper, "A new coplanar-grid high-pressure xenon gamma-ray spectrometer," *IEEE Trans. Nuclear Sci.*, vol. 52, no. 6, pp. 2932–2939, Dec. 2005.

[81] T. van Vuure, C. van Eijk, F. Fraga, R. Hollander, and L. Margato, "High-pressure GEM operation aiming at thermal neutron detection," *IEEE Trans. Nuclear Sci.*, vol. 48, no. 4, pp. 1092–1094, Aug. 2001.

[82] J. Veloso, F. Amaro, J. Santos, J. Mir, G. Derbyshire, R. Stephenson, N. Rhodes, and E. Schooneveld, "Application of the microhole and strip plate detector for neutron detection," *IEEE Trans. Nuclear Sci.*, vol. 51, no. 5, pp. 2104–2109, Oct. 2004.

[83] G. Charpak, R. Bouclier, T. Bressani, J. Favier, and C. Zupancic, "The use of multiwire proportional counters to select and localize charged particles," *Nuclear Instum. Method*, vol. 62, no. 3, pp. 262–268, Jul. 1968.

[84] A. Oed, "Position-sensitive detector with microstrip anode for electron multiplication with gases," *Nuclear Instrum. Methods Phys. Res. A.*, vol. 263, nos. 2–3, pp. 351–359, 1998.

[85] T. Francke and P. Vladimir, "Micropattern gaseous detectors," in *Proc. 17th Int. Workshop Vertex Detect.*, Sep. 2003, p. 38.

[86] G. Charpak, J. Derre, Y. Giomataris, and P. Rebourgeard, "Micromegas, a multipurpose gaseous detector," *Nuclear Instrum. Methods Phys. Res.*, vol. 478, nos. 1–2, pp. 26–36, Feb. 2002.

[87] A. Sarvestani, H. Besch, M. Junk, W. MeiBner, N. Pavel, N. Sauer, R. Stiehler, A. Walenta, and R. Menk, "Gas amplifying hole structures with resistive position encoding: A new concept for a high rate imaging pixel detector," *Nuclear Instrum. Methods Phys. Res.*, vol. 419, nos. 2–3, pp. 444–451, Dec. 1998.

[88] F. Sauli, "Gas detectors: Achievements and trends," *Nuclear Instrum. Methods Phys. Res. A*, vol. 461, nos. 1–3, pp. 47–54, 2001.
[89] F. Sauli, "Micro-pattern gas detectors," *Nuclear Instrum. Methods Phys. Res. A*, vol. 477, nos. 1–3, pp. 1–7, Jan. 2002.
[90] A. Breskin, "Advances in gas avalanche radiation detectors for biomedical applications," *Nuclear Instrum. Methods Phys. Res.*, vol. 454, no. 1, pp. 26–39, 2000.
[91] W. R. Hendee and E. R. Ritenour, *Medical Imaging Physics*, 4th ed. New York: Wiley, 2002.
[92] T. Fawcett, "An introduction to ROC analysis," *Pattern Recognit. Lett.*, vol. 27, no. 8, pp. 861–874, 2006.
[93] C. D. Brown and H. T. David, "Receiver operating characteristics curves and related decision measures: A tutorial," *Chem. Intell. Lab. Syst.*, vol. 80, no. 1, pp. 24–38, 2006.
[94] R. Kyker, N. Berry, D. Stark, N. Nachtigal, and C. Kershaw, "Hybrid emergency radiation detection: A wireless sensor network application for consequence management of a radiological release," *Proc. SPIE*, vol. 5440, no. 1, pp. 293–304, 2004.
[95] R. J. Nemzek, J. S. Dreicer, D. C. Torney, and T. T. Warnock, "Distributed sensor networks for detection of mobile radioactive sources," *IEEE Trans. Nuclear Sci.*, vol. 51, no. 4, pp. 1693–1700, Aug. 2004.
[96] J. Brittain, "Electrical engineering hall of fame: Guglielmo marconi," *Proc. IEEE*, vol. 92, no. 9, pp. 1501–1504, Aug. 2004.
[97] A. Heaton and J. Reeves, "Microwave radiation from discharges," in *Proc. 3rd Int. Conf. Gas Discharges*, 1974, pp. 73–77.
[98] C. K. Eun, R. Gharpurey, and Y. B. Gianchandani, "Wireless signaling of beta detection using microdischarges," *J. Microelectromech. Syst.*, vol. 19, no. 4, pp. 785–793, Aug. 2010.
[99] C. K. Eun and Y. B. Gianchandani, "A bulk silicon micromachined structure for gas microdischarge-based detection of beta-particles," *J. Micromech. Microengin.*, vol. 18, no. 9, 10 pp. 95007-1–95007-10, Sep. 2008.

Christine K. Eun received the B.S. (*summa cum laude*), M.S., and Ph.D. degrees from the University of Michigan, Ann Arbor, in 2004, 2006, and 2011, respectively, all in electrical engineering.

She has been funded through various fellowships, including the Rackham Merit Fellowship and a fellowship from Sandia National Laboratories.

Yogesh B. Gianchandani (F'10) is a Professor at the University of Michigan, Ann Arbor, with a primary appointment in the Electrical Engineering and Computer Science Department and a courtesy appointment in the Mechanical Engineering Department. He also serves as the Director for the Center for Wireless Integrated MicroSensing and Systems (WIMS^2).

Dr. Gianchandani's research interests include all aspects of design, fabrication, and packaging of micromachined sensors and actuators (http://www.eecs.umich.edu/ yogesh/). He has published about 250 papers in journals and conferences, and has about 30 US patents issued or pending. He was a Chief Co-Editor of *Comprehensive Microsystems: Fundamentals, Technology, and Applications*, published in 2008. From 2007 to 2009 he also served at the National Science Foundation, as the program director for Micro and Nano Systems within the Electrical, Communication, and Cyber Systems Division (ECCS).